



**HAL**  
open science

## Innovative polypropylene based blends by in situ polymerization of a polyimide dispersed phase by reactive extrusion

Charlotte Dubois, C. Marestin, Philippe Cassagnau, Karim Delage, Pierre Alcouffe, Nicolas Garois, Véronique Bounor-Legaré

### ► To cite this version:

Charlotte Dubois, C. Marestin, Philippe Cassagnau, Karim Delage, Pierre Alcouffe, et al.. Innovative polypropylene based blends by in situ polymerization of a polyimide dispersed phase by reactive extrusion. *Polymer*, 2022, 254, pp.125022. 10.1016/j.polymer.2022.125022 . hal-03759559

**HAL Id: hal-03759559**

**<https://hal.science/hal-03759559v1>**

Submitted on 24 Aug 2022

**HAL** is a multi-disciplinary open access archive for the deposit and dissemination of scientific research documents, whether they are published or not. The documents may come from teaching and research institutions in France or abroad, or from public or private research centers.

L'archive ouverte pluridisciplinaire **HAL**, est destinée au dépôt et à la diffusion de documents scientifiques de niveau recherche, publiés ou non, émanant des établissements d'enseignement et de recherche français ou étrangers, des laboratoires publics ou privés.

# Innovative polypropylene based blends by *in situ* polymerization of a polyimide dispersed phase by reactive extrusion

Charlotte Dubois<sup>1,3</sup>, Karim Delage<sup>1</sup>, Pierre Alcouffe<sup>1</sup>, Nicolas Garois<sup>2</sup>, Catherine Marestin<sup>1</sup>, Philippe Cassagnau<sup>1</sup>, Véronique Bounor-Legaré<sup>1\*</sup>

1 : Univ de Lyon, CNRS, UMR 5223, Ingénierie des Matériaux Polymères, Université Claude Bernard Lyon 1, F-69622, Villeurbanne, France

2 : Centre de recherche Hutchinson, rue Gustave Nourry BP31, 45120, Chalette-sur-Loing, France

3 : TotalEnergies, Tour Coupole La Défense, 2 place Jean Millier, 92078, Paris, France

\*: corresponding author, [veronique.bounor-legare@univ-lyon1.fr](mailto:veronique.bounor-legare@univ-lyon1.fr)

**Keywords:** reactive extrusion, polymer blends, mechanical reinforcement, polyimide

## Abstract

Polypropylene/polyimide (PP/PI) blends were synthesized by reactive extrusion with the *in situ* polymerization of the polyimide phase in presence of maleic anhydride grafted polypropylene (PP-g-MA) as a compatibilizer. Blends were reactively processed in a twin-screw extruder at 200°C, with the PI content varying from 10 to 40 wt%. Examination of morphology by scanning electron microscopy (SEM) depicted a fine sub-micrometer dispersion of the polyimide phase ranging from 170 to 250nm in diameter, for all PI concentrations. The advantage of the *in situ* approach compared to the more classical dispersion process was clearly demonstrated. The *in situ* synthesized PI phase was characterized by NMR and FTIR after separation by Soxhlet selective extraction. Differential scanning calorimetry (DSC) analysis of the blends showed no modifications of PP's crystallinity with the addition of PI. Rheological behaviors showed a significant impact of the polyimide phase on the storage modulus with the appearance of a secondary storage modulus plateau at low frequencies. Thermogravimetric analyses evidenced an improvement of the thermal stability of the blends, with an increase of the decomposition temperature up to 35°C depending on the polyimide content. Mechanical properties were also improved due to the high mechanical strength of the polyimide phase, with an increase in Young's modulus up to +35% for the highest polyimide content.

## Introduction

Polypropylene (PP) is a semi-crystalline polymer with very attractive properties such as high chemical resistance, low water permeability, good melt processability and low-cost. PP is one of the most widely used commercial commodity polymers, in a large field of applications ranging from packaging to electronics. However, because of its low melting temperature and poor heat resistance, PP cannot be employed in certain high-performance applications. To overcome this drawback, there is a

growing interest in blending polypropylene with polymers presenting for example a higher heat resistance, in order to reach a unique balance of performance/cost ratio and further upgrade its range of applications.

Melt blending PP with specialty or engineering polymers has been investigated in the past. To illustrate, the following researches on PP blends can be cited: i) PP/Polycarbonate, ii) PP/Poly(phenylene oxide) and iii) PP/Poly(ether sulfone):

i) Polycarbonate (PC) is an engineering polymer with good mechanical strength and temperature resistance [1-4]. Renault and coworkers [1] studied the thermal and morphological behavior of melt processed PP/PC 75/25 wt% blends. The blends were melt-mixed at 230°C in an internal mixer for 10 minutes, which led to a dispersion of 5µm in diameter PC particles in the PP matrix. The thermal properties of the PC phase led to a 20°C increase of the maximal decomposition temperature of the PP/PC blend.

ii) Poly(phenylene oxide) (PPO) is a high performance polymer with a high glass transition temperature ( $T_g = 215^\circ\text{C}$ ), low water absorption, good dimensional stability and high ductility [5]. Despite its attractive properties, PPO itself has very limited applications due to its brittleness and poor processability but many thermoplastics/PPO blends have been developed to combine the easy-processability of the chosen thermoplastics with the outstanding properties of PPO. More specifically, PPO has been used to improve the temperature resistance of polypropylene [6-9]. For example, Oyama *et al.* [6] improved the decomposition temperature of polypropylene by 30°C for PP/PPO 60/40 wt% blends prepared in a conical twin screw extruder at 280°C. They were able to reach a distribution of 0.3µm PPO domains in the PP matrix, with the addition of styrene-ethylene-butylene-styrene (SEBS) as a compatibilizer. Paszkiewicz and coworkers [7] studied the thermal properties of melt blended PP/PPO (80/20 wt%) blends in a twin screw extruder at 290°C and also noticed a 20°C increase of PP's thermal stability.

iii) Poly(ether sulfone) (PES), another high performance polymer with a high heat deflection temperature (200°C), was also blended with polypropylene by Oyama *et al.* [10]. They added 20 wt% of PES in the PP matrix with glycidyl methacrylate-grafted PP as a compatibilizer by melt mixing at 300°C under nitrogen atmosphere. They observed PES domain size of 1-3µm, and an improvement of 20°C in the temperature at 5wt% mass loss.

Like PPO and PES, polyimides (PI) are a type of thermostable polymers which exhibit very attractive properties. PI have excellent thermal, mechanical and dielectric properties with good chemical resistance and dimensional stability. They have found applications in many technologies including microelectronics, high temperature adhesives or gas separation membranes. They have been blended in the past with other polymers to bring new properties to polymers. For example, the commercial polyetherimide YZPI™ from Nanjing Yuezi ( $T_g=255^\circ\text{C}$ ) was blended by Gao *et al.* [11] with poly(ether ketone) (PEEK) in order to obtain high dielectric constant composites. Liu and coworkers [12] have incorporated 1 to 7 wt% of a commercial thermoplastic polyimide GCPI™-M1 (TPI) in a polyamide 66 matrix in a twin-screw extruder at 270°C. Thanks to the high  $T_g$  of the TPI (250°C), the blends exhibited a higher heat distortion temperature, with a maximum increase of 7°C for 3 wt% of TPI.

One of the major problems of polyimides is their poor processability. Indeed, many of them in their full imidized forms are insoluble in common organic solvents and mostly infusible at elevated processing temperatures. There are therefore limitations for conventional melt blending polyimides with other polymers, and the range of suitable polyimides is restricted by their glass transition temperatures. To overcome those issues, blends can be prepared through reactive extrusion based on the *in situ* polymerization of a minor phase in a thermoplastic matrix [13, 14].

Specifically, in the case of polypropylene, this method has been used to polymerize *in-situ* a reinforcing polymer in the matrix. Hu and Cartier [15] prepared PP/PA6 blends in a twin-screw extruder by *in situ* polymerizing  $\epsilon$ -caprolactam. This synthesis was realized in the presence of a fraction of PP chains bringing 1.1 wt% isocyanate groups (PP-g-TMI), which act as a macroactivator for the  $\epsilon$ -caprolactam polymerization and to form a graft copolymer of PP and PA6 at their interface. PP/ $\epsilon$ -CL/NaCl/microactivator 50/50/3/3 wt% and PP-g-TMI/ $\epsilon$ -CL/NaCl/microactivator 50/50/3/3 wt% blends were prepared in a co-rotating twin-screw extruder at 240°C under a nitrogen purge. The blends prepared with PP-g-TMI displayed a remarkable elongation at break of 142% with a testing speed of 500mm/min. The size of the particles of the PA6 dispersed phase was between 10 and 100 nm, which could not have been achieved by simple melt blending. Indeed, the morphology formed by polymerization-induced separation led to a very fine dispersion. Teng *et al.* [16] also developed PP/PA6 blends with the *in situ* synthesis of the polyamide phase through anionic polymerization of  $\epsilon$ -caprolactam. Several PP/PA6 blends in the composition range 60/40 to 40/60 wt% were prepared in an internal mixer at 230°C. The domain size of PA6, dispersed in the PP matrix, was found to be considerably smaller than that in classical melt blending of PP and premade PA6. The PA6 particle size was reduced from  $>2\mu\text{m}$  to  $<0.5\mu\text{m}$  in the presence of the compatibilizing agent PP-g-MA. More recently in our group, Barroso Gago *et al.* [17] developed PP/PP-g-MA/thermoset blends with the *in situ* synthesis of the epoxy based thermoset phase in a twin-screw extruder at 200°C. The thermoset phase (TS) was well dispersed in the PP matrix, with TS domains around 0.5  $\mu\text{m}$  in diameter. The high mechanical strength of the thermoset phase led to a 24% increase in Young's modulus. The resilience of the material was also improved due to the apparition of a  $\beta$ -crystalline phase in PP, which was proved to be generated from the *in situ* synthesis of the TS phase.

Actually, these reactive processing approaches represent an elegant way to develop well-defined structures of polymer blends at the micro- and nanoscale [15-19] and are compatible with the incorporation of high Tg polymers. Moreover, a recent study by Verny *et al.* [20] explored the synthesis of polyimides in a solvent-free process in a twin-screw extruder. They were able to synthesize a polyimide from pyromellitic dianhydride (PMDA) and Jeffamine D-230, with a complete imidization in less than 5min at 200°C in the molten state. It is then conceivable to use reactive processing to create PP/PI blends with the *in-situ* synthesis of the polyimide phase. Compared to classical melt blending, reactive extrusion offers a lot more possibilities in terms of polyimide structures. Indeed, many commercial precursors are available and can be combined to tailor the structure of the *in situ* synthesized polyimide.

Based on these concepts, we propose in this study to create new polypropylene/polyimide blends by the *in situ* synthesis of the polyimide dispersed minor phase. PP/PI blends were reactively processed in a twin-screw extruder, with the concentration of PI varying from 10 to 40 wt%. The goal of this study is to demonstrate the possibility to create a polyimide structure *in situ* in a molten continuous process. This work will investigate the chemical and morphological structures related to the

improvement of polypropylene's properties with the *in situ* creation and compatibilisation of the polyimide phase.

## Materials and formulations

### 1. Materials

The polypropylene matrix PPH3060 with a melt flow index of 1.8 g/10 min (at 230°C, 2.16 kg) and a zero shear viscosity  $\eta_0=700$  Pa.s at 200°C was kindly supplied by Total as polymer pellets. Maleic anhydride grafted polypropylene Exxelor PO1020 (MA level 1.2 wt%), with a melt flow index of 430 g/10 min (at 230°C, 2.16 kg) was purchased from ExxonMobil as polymer pellets. Pyromellitic dianhydride (PMDA) and trimethylhexanemethylenediamine (TMD) were purchased from TCI Chemicals and used as received. N,N-Dimethylformamide, 1,1,1,3,3,3-Hexafluoro-2-propanol and N-methyl-2-pyrrolidone (NMP) were purchased from Sigma Aldrich and used as received. Table 1 depicts the main characteristics of these materials.

Table 1 : Main physical and chemical characteristics of the materials

Name	Commercial Name	M (g/mol)	Tm (°C)	Tb (°C)	Density (g/cm <sup>3</sup> )
PP	PPH3060	Mn : 72,000 Mw : 384,000	165	/	0.9
PP-g-MA*	PO 1020	Mn : 36,000 Mw : 91,000	162	/	0.9
PMDA	Pyromellitic dianhydride	218.12	285	400	1.68
TMD	Trimethylhexanemethylenediamine	158.28	-80	232	0.87

\*: Maleic anhydride grafting rate of 1.2wt% (checked by acid-base titration)

### 2. Synthesis of polyimides

For better understanding, the pure polyimide was synthesized in solution from two non-toxic monomers. Pyromellitic dianhydride (PMDA) is a commercial dianhydride extensively used in the synthesis of commercial polyimides such as Kapton® and well known to confer a highly rigid structure to the resulting polymers (Tg = 385°C and Td5% = 608°C for Kapton®). The diamine is a mixture of (2,2,4) and (2,4,4) trimethylhexanemethylenediamine (TMD) (two flexible aliphatic diamine isomers produced by Evonik). The incorporation of these diamines in the polyimide structure (displayed in Figure 1) was expected to bring flexibility to the polymer chains.

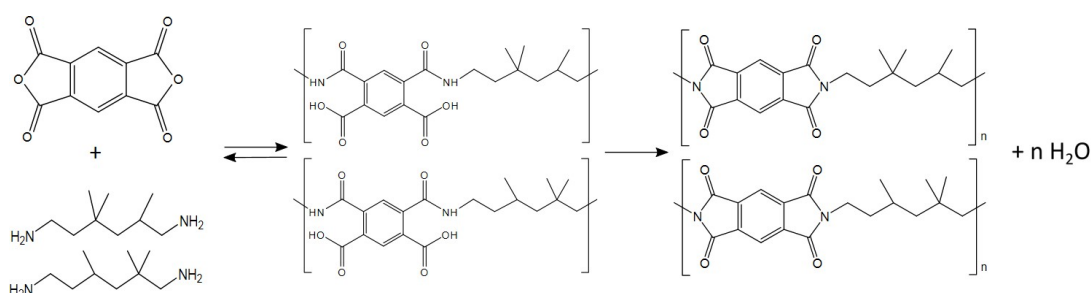


Figure 1 : Chemical structures of the synthesized polyimide

### 2.1. Synthesis in solution

In a three-neck round bottom flask equipped with a nitrogen inlet and a mechanical stirrer, an equimolar amount (13,75mmol) of dianhydride and diamines were suspended in 12 mL of m-cresol (30 wt%). The reaction mixture was heated at 180°C for 6 hours. The highly viscous solution was poured into methanol. The fibrous polymer was isolated by filtration and crushed. After purification by Soxhlet extraction with methanol, the polymer was dried overnight under vacuum at 80°C.

### 2.2. Bulk synthesis in a micro-extruder

The polyimide was synthesized in an Xplore DSM vertical microextruder (14 cm<sup>3</sup> capacity) equipped with twin conical screws. This device allows the recirculation of the melt polymer, which can be used to tailor the extrusion time. The polyimide was synthesized in two steps: stoichiometric amounts of dianhydride and diamine were preliminary mixed by simple grinding. The resulting poly(amic acid) was then introduced in the micro-extruder to achieve the imidization reaction and form the polyimide. The rotation speed was set at 50 rpm and the temperature at 250°C. Aliquots of the extrudate were collected at different reaction times and further analyzed using FTIR, DSC and NMR.

## 3. Synthesis of PP/PI blends

### 3.1 Simple melt blending

A PP/PP-g-MA/PI 40/30/30 wt% blend was prepared by simple melt blending in an Xplore DSM vertical microextruder equipped with twin conical screws. The polyimide incorporated in the blend was previously synthesized in bulk in the microextruder. PP, PP-g-MA and pre-synthesized PI were added simultaneously into the microextruder. The rotation speed was set at 100rpm and the temperature at 200°C.

### 3.2. In situ synthesis by reactive blending

Different blends were synthesized by melt-blending in a co-rotating twin-screw extruder (Leistritz ZSE18HPe-60D model, diameter 18 mm, L/D=60) at 200°C and screw speed of N=600 rpm. The twin-screw profile is shown in Figure 2. It particularly contains two reverse conveying elements: the first one is positioned (L/D=15) upstream of the diamine injection (L/D=17.5) to avoid the liquid from rising out, and the second one is positioned (L/D=45) at two thirds of the extruder to create a plug upstream of the evaporation of the volatiles.

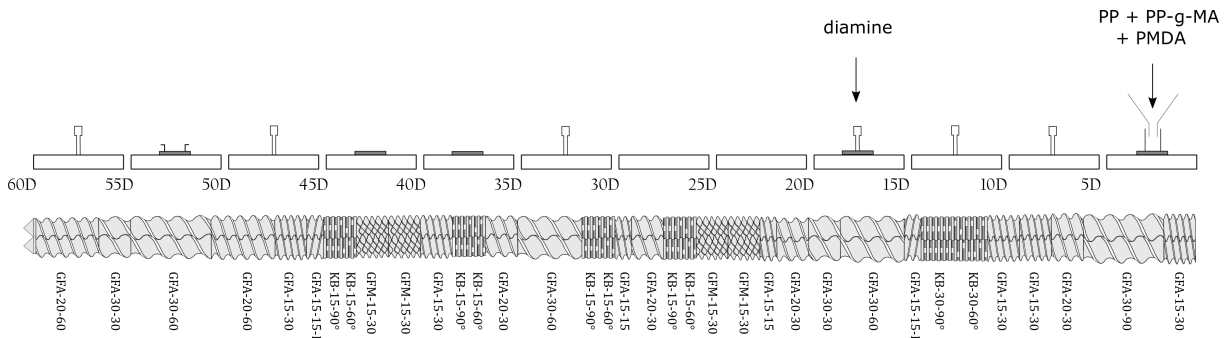


Figure 2 : Twin-screw profile with two reverse conveying elements

Different polyimide contents were *in situ* synthesized in the polypropylene based matrix by adding stoichiometric amounts of dianhydride and diamine. The flow rates of the different components were adapted for every formulation to maintain a total extrusion flow rate of  $Q=3$  kg/h. A description of all the formulations is referenced in Table 2. PP, PP-g-MA and PMDA were incorporated by the main hopper, whereas TMD was incorporated in the matrix in the molten state at the injection point  $L/D=17.5$  using an external liquid pump. For the PP/PP-g-MA reference blends, no PMDA or TMD was added in the extruder. Similarly, for the PP/*in situ* PI blends (without PP-g-MA), only PP was incorporated by the hopper, but the polyimide was synthesized in the same way. The final barrel element at  $L/D=57.5$  was kept open to evaporate the water created during the polycondensation reaction. The mean residence time of the polymer in the extruder was calculated at 90 seconds under those processing conditions using the Ludovic software. At the end of the extruder, samples were cooled down with air and granulated.

Table 2 : Blend compositions in weight % and corresponding extrusion flow rates (kg/h)

	Composition in wt%		
	PP	PP-g-MA	PI
<b>Reference blends</b>	100	-	-
	90	10	-
	80	20	-
	70	30	-
	60	40	-
<b>PP/PP-g-MA/ in situ PI blends</b>	80	10	10
	60	20	20
	40	30	30
	20	40	40
<b>PP/in situ PI blend</b>	70	-	30

After extrusion, the pellets of the different blends were injected in a hydraulic injection molding machine Babyplast 6/10P equipped with a 14mm diameter piston and presenting a clamping force of 62 kN. Injected samples were either dog boned shaped H2 samples for tensile testing or cylindrical samples (25 mm in diameter, 2 mm thick) for rheological measurements. Chamber temperature was set at 200°C, mold temperature at 40°C and the injection pressure was adapted to each sample to provide an optimal filling of the mold.

For some specific characterization the polyimide phase was extracted from the polypropylene matrix (previously grinded as a fine powder) by a 48h Soxhlet extraction with dimethylformamide (DMF). After elimination of the solvent by evaporation, the polyimides were dried overnight under vacuum at 80°C.

## Methods of characterization

### Chemical characterizations

## FTIR

Fourier-transform infrared spectroscopy (FTIR) ranging from 650 to 4000  $\text{cm}^{-1}$  was recorded on a Nicolet IS10 machine, in attenuated total reflectance (ATR) mode, with 64 scans for each sample.

## Nuclear Magnetic Resonance (NMR)

$^{13}\text{C}$  liquid-state NMR analyses were performed on a Bruker Avance II spectrometer working at 100.6 MHz with a 10mm  $^1\text{H}/^{13}\text{C}$  selective probe. The samples were analyzed in HFIP/ $\text{CDCl}_3$  (80/20 v/v) at 25°C with concentrations of 100 mg/mL. The chemical shifts were referenced to tetramethylsilane used as the internal standard ( $\delta = 0\text{ppm}$ ).

## Size Exclusion Chromatography (SEC)

Size exclusion chromatography measurements were carried out on an Acquity Advanced Polymer Chromatography System. Samples were dissolved in HFIP to obtain 5g/L solutions. The signals were detected using a refractive index detector (Waters RI detector). Number-average ( $M_n$ ), weight-average ( $M_w$ ) and dispersities were obtained from a calibration curve based on poly(methylmethacrylate) standards.

### Morphological characterizations

## Scanning Electron Microscopy (SEM) and Transmission Electron Microscopy (TEM)

Scanning electron microscopy (SEM) observations were carried out on a FEI Quanta 250 electron microscope using an acceleration voltage of 10 kV and under high vacuum. A flat surface of specimens was obtained with an ultramicrotome UC7 Leica at room temperature using an oscillating diamond knife (Diatome). In order to contrast the two phases, the samples were stained for 48 h in a 50:50 water:sodium hypochlorite solution with 2 wt% of ruthenium tetroxide ( $\text{RuO}_4$ ).  $\text{RuO}_4$  preferentially stains the polyimide phase, which appears lighter than polypropylene due to the heavy Ru element. After staining, the samples were thoroughly rinsed with distilled water and then microtomed to an optimal depth of 0.5  $\mu\text{m}$ . The samples were sputter-coated with a 10 nm layer of carbon to ensure a good electrical conductivity between the surface of the sample and the specimen holder. While microtoming, ultrathin sections of 80 nm were collected for Transmission Electronic Microscopy (TEM) on a copper grid and were observed on a Philips CM120 microscope operating at 80 kV. In this case, the polyimide phase appears darker than polypropylene.

### Thermal characterizations

## Differential Scanning Calorimetry

Thermal properties of the formulations were characterized by differential scanning calorimetry (DSC) to study the melting and crystallization behavior using a model Q200 (TA Instruments) equipped with a cooling system 90. Indium was used as a calibration standard. 5 to 10 mg of the samples were weighed and placed into hermetic aluminum capsules. The value of the melting temperature ( $T_m$ ), crystallization temperature ( $T_c$ ) and enthalpy were measured on the first cycle applied from -50°C to 250°C at a heating rate of 10°C/min under nitrogen. The degree of crystallinity was calculated with the equation as follows:

$$\chi_c = \frac{\Delta H_m}{\Delta H_m^0(1 - \Phi)} \quad \#Eq. 1$$

Where  $\Phi$  is the weight fraction of PI in blend,  $\Delta H_m$  is the sample melting enthalpy and  $\Delta H_m^0$  is the melting enthalpy of 100% crystalline PP ( $\Delta H_m^0$  PP = 209 J/g [21]).

#### X-ray diffraction: Wide Angle X-ray Scattering (WAXS)

The measurements were carried out at the European Synchrotron Radiation Facility (ESRF, Grenoble, France) on the D2AM beamline. The incident photon energy was set at 16 keV and a IMXPAD WOS-S700 2D detector was used for WAXS measurements. The sample-to-detector distance was about 9.74 cm and the beam stop had a 1 mm diameter. The  $q$ -calibrations were achieved using lanthanum hexaboride standards. The intensity calibration was performed using a glassy carbon standard. Each sample was hot pressed into a 200 to 300  $\mu\text{m}$  thick film without any preferential orientation and placed into sample holders. The intensity from the samples was obtained by taking into account the detector geometry and flat-field response, by normalization from the thickness and attenuation of the samples and by subtraction of the intensity of the empty cell. The corrected two-dimensional data were averaged azimuthally to obtain intensity  $I$  vs scattering vector  $q$  ( $q = (4\pi/\lambda)\cdot\sin(\vartheta)$ , where  $2\vartheta$  is the scattering angle and  $\lambda$  is the incident wavelength).

#### Thermo Gravimetric Analysis

Decomposition temperature was measured by Thermo Gravimetric Analysis (TGA) on a TGA Q500 (TA Instruments). Approximately 10 to 15 mg samples were placed in a platinum crucible and heated from 30°C to 550 °C at 10°C/min in a controlled inert atmosphere (helium) or were heated up to 400°C at 10°C/min followed by a 2 h isotherm at 400°C.

#### Rheological characterization

Dynamic frequency tests were conducted on a strain-controlled Discovery Hybrid Rheometer DHR (TA Instruments) using a parallel plate geometry (25 mm diameter, 2 mm gap). Measurements were performed at 220°C under a nitrogen flow to prevent thermal degradation. The complex shear modulus was then measured (storage modulus  $G'(\omega)$  and loss modulus  $G''(\omega)$ ) by varying the frequencies from 100 to 0.01 rad/s in the linear regime.

#### Mechanical characterizations

##### Tensile testing

Uniaxial tensile tests were performed on a Shimadzu AG-X tensile testing machine equipped with a load cell of 10kN at room temperature. To comply with ISO-527-2 standard, each blend was tested at a speed of 50m/min to measure yield stress and elongation at break and at 1mm/min to determine Young's modulus. At least 8 different samples were tested for each formulation, until a satisfactory standard deviation was obtained.

## Results and discussion

## Bulk polyimide synthesis

PI was synthesized in bulk conditions in a microextruder in order to evaluate the reactions conversion and properties related to the experimental conditions encountered in an extruder. A dianhydride/diamine stoichiometric premix was preliminary prepared, by thoroughly mixing the two monomers. The formation of poly(amic acid) species is confirmed by FTIR analysis, as reported in Figure 3. The bands initially present at  $1695\text{ cm}^{-1}$  and  $1765\text{ cm}^{-1}$ , characteristic of PMDA C=O stretching, disappeared in the FTIR spectrum of the premix system. They were replaced by a band at  $1570\text{ cm}^{-1}$ , attributed to the aromatic ring stretching of amic/acid groups, and a band at  $1365\text{ cm}^{-1}$ , attributed to the amide C-N stretching. The apparition of a broad band at  $3300\text{ cm}^{-1}$  indicates the presence of a carboxylic acid group (OH vibration), further confirming the formation of a poly(amic acid) structure in the dianhydride/diamine premix. The poly(amic acid) structure has also been confirmed by  $^{13}\text{C}$  NMR analysis (spectrum available in S1).

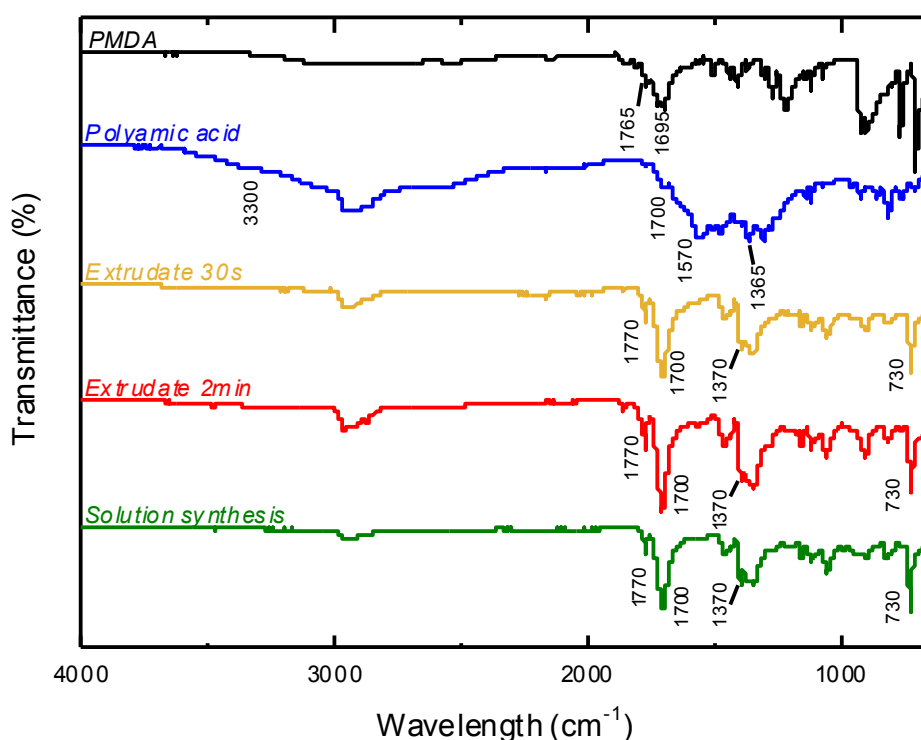


Figure 3 : FTIR spectra of PMDA, poly(amic acid), PI after 30s and 2 min of bulk synthesis in a microextruder at  $250^{\circ}\text{C}$  and PI synthesized in solution

FTIR spectra of the extruded polyimide at different reaction times are displayed in Figure 3. The signatures of an imidization reaction (amic acid cyclization in an imide group and release of a water molecule, as described in Figure 1) are present as soon as 30 seconds of reaction. Indeed, the absorption bands observed at  $1700\text{ cm}^{-1}$  and  $1770\text{ cm}^{-1}$  correspond respectively to the asymmetric and symmetric stretching of C=O in the imide ring. The imide C-N stretching vibration at  $1370\text{ cm}^{-1}$  and the imide ring bending at  $730\text{ cm}^{-1}$  confirm the formation of a polyimide structure. The same characteristic bands are found in the extrudate's spectrum at  $t=2\text{min}$ , showing that the chemical structure does not evolve substantially with the reaction time and that it is stable from 30 seconds of reaction. Moreover, the extrudate's spectrum is identical to the one of PI synthesized in solution, which corroborates the formation of the desired polyimide structure. The chemical structure was also confirmed by  $^{13}\text{C}$  NMR analysis (spectra available in S2). The glass transition temperature of the

polyimide synthesized by both techniques was compared and found to be very similar (155°C for the PI synthesized in bulk in the microextruder and 160°C for the PI synthesized in solution).

## PP/PI synthesis

### Chemical characterization of the *in situ* polymerized polyimide

As detailed previously, several concentrations of polyimide were *in situ* synthesized in the polypropylene based matrix using a twin-screw extruder (formulations in Table 2). After Soxhlet extraction in DMF of the *in situ* synthesized PP/PP-g-MA/PI 40/30/30 blend, some macromolecular material was isolated and characterized by FTIR, NMR spectroscopy and SEC. The experimental proportion of extracted polyimide (67% of the theoretical incorporated PI in the blend) shows that a significant amount of PI could not be extracted, probably because it has been covalently grafted onto PP-g-MA during reactive extrusion. Anyhow, the analyses evidenced the structure of a polyimide (S4 and S5). While lower than molar mass of a polyimide synthesized in solution (Table 3), the molar mass of the polyimide formed *in situ* in PP by reactive extrusion is quite high (19,000 g/mol, DP<sub>n</sub>=50) and such values can be considered as high molar mass polycondensate.

The *in situ* polymerization in a polyolefin matrix and in presence of PP-g-MA could explain the difference in molar mass compared to the solution synthesis. The maleic anhydride groups brought by the compatibilizer can react with the polyimide in growth and thus modify the expected chain length. Moreover, the presence of PP-g-MA creates a stoichiometry deviation due to the maleic anhydride functions (0.7wt% in PP-g-MA). To evaluate the impact of this deviation on the molar mass, Carothers equation (Eq.3) can be used. This equation is valid when the degree of conversion  $p \rightarrow 1$ , with DP<sub>n</sub> the number of repeating units and  $r$  the stoichiometry deviation (inferior to 1).

$$DP_n \rightarrow \frac{(1+r)}{(1-r)} \quad \#Eq.2$$

From the experimental SEC DP<sub>n</sub> value (Table 3) of the polyimide synthesized in solution, the stoichiometric deviation of the two monomers in a diluted environment can be calculated at  $r=0.994$  and taken as a reference for this polymerization. For the polyimide synthesized *in situ* in molten PP in presence of PP-g-MA, the molar mass of maleic anhydride coming from PP-g-MA leads to a higher stoichiometry deviation with  $r=0.968$ . From Eq.3, this stoichiometry ratio would theoretically form a polymer with DP<sub>n</sub>=62 and Mn=23,000 g/mol. These theoretical values are close to the ones obtained experimentally after Soxhlet extraction of the polyimide synthesized *in situ* (DP<sub>n</sub>=50, Mn=19,000 g/mol). These calculations highlight that the molar masses achievable by reactive extrusion are lower than those obtained in solution due to the stoichiometry deviation in presence of PP-g-MA.

Table 3: DSC and SEC analysis of PI synthesized in solution and PI synthesized *in situ* via reactive extrusion in PP, after Soxhlet extraction

Synthesis	Tg (°C)	Mn (g.mol <sup>-1</sup> )	Mw (g.mol <sup>-1</sup> )	Polydispersity	DP <sub>n</sub>
Solution	160	62,000	147,000	2	165
Reactive extrusion	138	19,000	47,000	2	50

The two polyimides' polydispersities are similar and equal to 2. For the synthesis *in situ* by reactive extrusion, this polydispersity value indicates that the dianhydride and diamine monomers are homogeneously dispersed in molten PP. A study by Cassagnau et al. [22] on polyethylene/polyurethane blends with the *in situ* synthesis of the polyurethane phase described that the low solubility of the alcohol monomers in molten PE led to a poor degree of polymerization and a high polydispersity. In contrast to this study, our experimental values suggest that the monomers have good solubility in molten PP throughout the extrusion, thus achieving the theoretical molar mass distribution of a polycondensate.

The two methods of polyimide synthesis led to a slight difference in glass transition temperatures. The T<sub>g</sub> of the PI synthesized *in situ* by reactive extrusion is lower than the one synthesized in solution (respectively 138°C and 160°C), which is probably due to its lower molar mass. Nevertheless, this *in situ* synthesized PI can be considered as a high T<sub>g</sub> polymer.

### Morphology development

For a comparison purpose of the reactive blending compared to classical melt blending, a blend with 30 wt% of pre-synthesized polyimide was elaborated in a microextruder. The morphology of this blend was compared to the one of the same blend made through reactive extrusion with the *in situ* synthesis of the polyimide phase. Scanning Electron Microscopy (SEM) images of the two blends are shown in Figure 4.

There is a significant morphology difference between the two ways of blending, as shown by a much finer dispersion of the PI particles with the *in situ* approach. The blend made through classical melt blending displays a broad PI particles' diameter distribution ranging from 500nm to 8µm, with a mean value of 1.9µm. The poor adhesion between the PI nodules and the PP matrix is evidenced in Figure 4a, as well as the presence of cracks that spread through the material during microtoming. These observations reveal the brittle behavior of the material made through classical melt blending. On the contrary, the PI particles' mean diameter is ten times smaller (180nm) with the *in situ* synthesis of the polyimide phase, and the blend's morphology is a lot more homogeneous (Figure 4b).

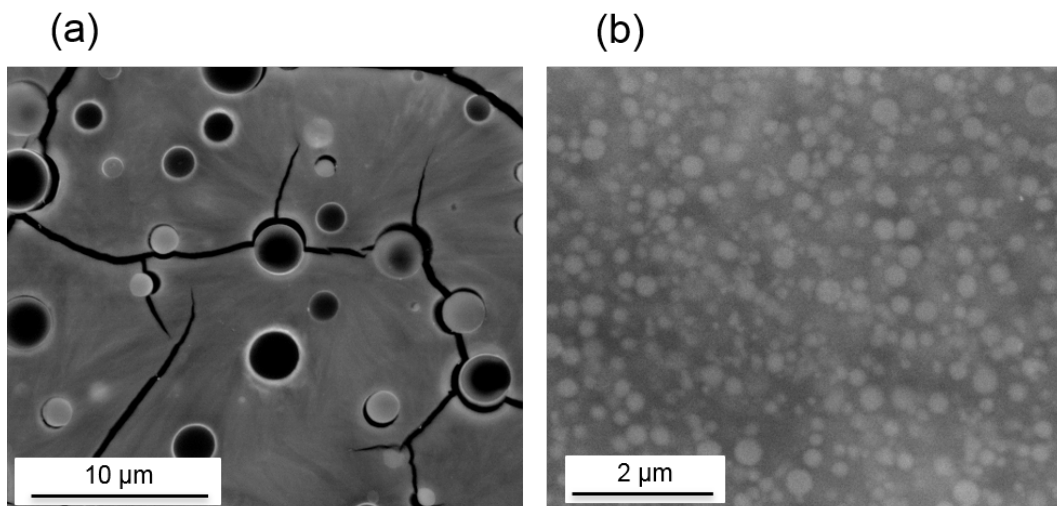


Figure 4 : SEM images of PP/PP-g-MA/PI blends (a) 40/30/30 melt blending and (b) 40/30/30 *in situ* synthesis

The same behavior has been observed by Kye and White [23] during their study of polyamide 6 (PA6) / polyether sulfone (PES) blends. They compared two processing techniques: the *in situ* polymerization of  $\epsilon$ -caprolactam during extrusion with PES and the simple mechanical blending of commercial PA6 with PES. Morphological analysis revealed that the dispersion of PES nodules was 10 times finer in the case of *in situ* polymerization. Similarly, Barroso Gago et al. [17] prepared PP/PP-g-MA/thermoset blends with the *in situ* synthesis of an epoxy based thermosetting phase by reactive extrusion. Thanks to the *in situ* synthesis, they observed a very fine dispersion of the thermoset phase in polypropylene with nodules of 0.5 $\mu\text{m}$  in diameter. The different mechanisms of the morphology development taking place in classical melt blending and *in situ* polymerization were explained by Hu and Cartier [15]. In the case of classical melt blending, the morphology comes from the reduction of the dispersed phase's size in the matrix. In the case of *in situ* polymerization, the morphology comes from the polymerization-induced phase separation. This explains why finer dispersions of the minor phase can be reached with its *in situ* polymerization.

To assess the efficiency of PP-g-MA, blends with 30wt% of PI were made with and without PP-g-MA. Morphology observations were performed to compare the dispersion of the polyimide phase in the polypropylene matrix and are displayed in Figure 5.

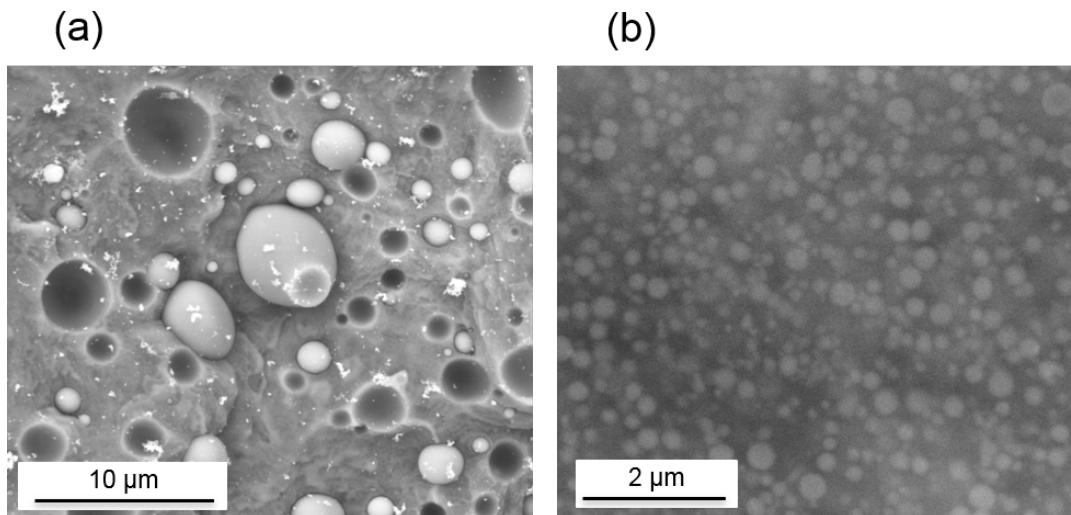


Figure 5 : SEM images of PP/PP-g-MA/*in situ* PI blends (a) 70/0/30 and (b) 40/30/30

There is a significant morphology difference between the two blends, with a much finer dispersion of the PI particles in presence of PP-g-MA. Indeed, without PP-g-MA, the polyimide particles have a distribution ranging from 400nm to 5 $\mu\text{m}$  in diameter, with a mean value of 1.7 $\mu\text{m}$ , which is 10 times larger than the mean value of PI particles in the formulation with PP-g-MA (180nm). The sample without PP-g-MA was cryogenically fractured in liquid nitrogen because the material was too brittle to be microtomed. As a result, voids can be observed in the blends without PP-g-MA at places where the PI nodules have been pulled off during the cryo-fracture. This phenomenon demonstrates a poor adhesion between the polyimide and the polypropylene matrix and the role of PP-g-MA. This result is consistent with the ones found in the literature dealing with the particle size reduction in polymer blends in the presence of maleated polypropylene [24-26].

The morphology development of the different PP/PP-g-MA/*in situ* PI blends was studied according to the created polyimide concentration as reported in Figure 6. The *in situ* synthesized polyimide phase appeared clearly and uniformly dispersed in the polypropylene based matrix. The polyimide nodules form sub-micrometer domains in the polypropylene matrix. The PI particles have a diameter distribution from 170 nm for smaller particles up to 250 nm, with a mean value of 210 nm for the four blends. The nodules' diameters are detailed for each PI concentration in Table 4. The increase of the polyimide concentration does not have a substantial effect on the polyimide nodules sizes at least in the concentration range investigated in the present study. Figure 7 shows the TEM images of PP/PP-g-MA/PI blends for three polyimide concentrations. It can be noticed that the polyimide nodules have a good adhesion to the polypropylene matrix, as no void between the nodules and the matrix are visible. The images reveal some presence of nodules aggregates for all concentrations. This morphological study justified the interest of synthesizing the polyimide phase *in situ* by reactive extrusion and the use of PP-g-MA as a compatibilizer.

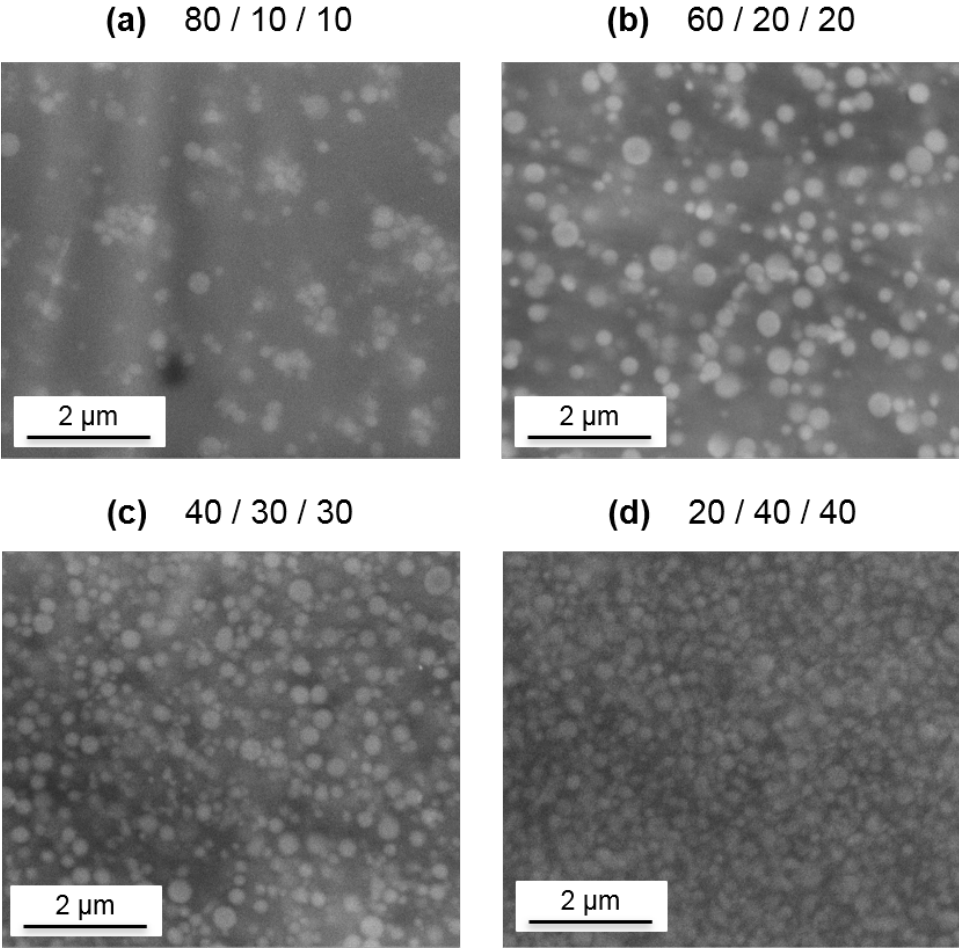


Figure 6 : SEM images of PP/PP-g-MA/PI (wt%) blends

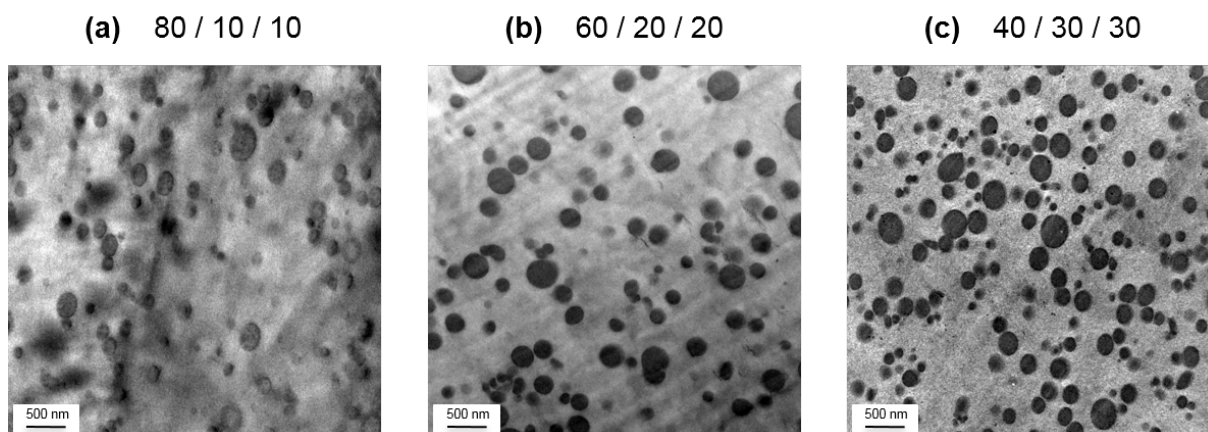


Figure 7 : TEM images of PP/PP-g-MA/PI (wt%) blends

The viscoelastic behavior of PP/PI blends as a function of angular frequency at 220°C is shown in Figure 8. For more clarity, only the results of the blends with 20% and 40% of polyimide are displayed. The behavior of the blends with 10 and 30% of PI is similar and can be found in S3. It can first be noted that both blends exhibit higher  $G'$  and  $G''$  values than their PP+PP-g-MA reference on the whole frequency range. The storage modulus increases with the PI content, which indicates that the blends become further elastic with the incorporation of polyimide. The storage modulus of the blends shows a second terminal relaxation zone at low frequencies. Furthermore, the dominance of the elastic behavior for these blends results in the appearance of a secondary plateau. The same phenomenon has been reported in the literature for blends having a nodular morphology. Sailer et al. [27, 28] were the first to propose an explanation for this particular rheological response. According to their work on compatibilized polyamide 6/styrene-acrylonitrile blends, they related the appearance of the secondary  $G'$  plateau to the creation of a three-dimensional network formed by the aggregation of the dispersed phase's particles. This network, with a high degree of interconnectivity, is responsible for the solid like behavior at low frequencies leading to apparent yield stress. This interconnectivity depends on many parameters including the volume fraction, the diameter of the dispersed phase's nodules and the interphase [29-32].

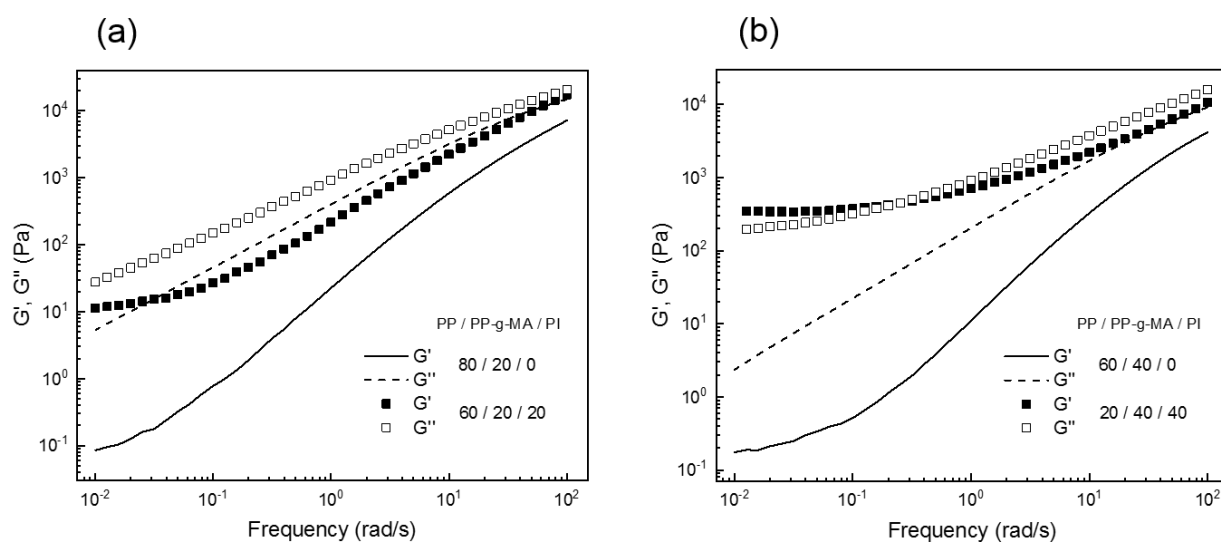


Figure 8 : Storage and loss modulus of PP/PP-g-MA/PI blends (a): 60/20/20, (b): 20/40/40 at 220°C under nitrogen

The inter-nodule distance  $d_i$  gives information on the degree of interaction between dispersed nodules. This parameter can be calculated from Equation 2 with the assumption that there is a simple cubic arrangement of monodisperse nodules [31]. In the equation  $d$  is the PI nodule diameter and  $V_i$  the volume fraction of the dispersed phase. The values of  $d_i$  are reported in Table 4.

$$d_i = d \left[ \left( \frac{\pi}{6 V_i} \right)^{1/3} - 1 \right] \quad \#Eq. 3$$

Interactions between nodules could occur if copolymers formed at the interface, from neighbor nodules, can entangle with each other. This phenomenon is considered to happen if the inter-nodule distance is lower than 1.5 times the radius of gyration ( $R_g$ ) of the copolymer grafted chain [32]. In our system, the anhydride functions of the PP-g-MA chains react and *in situ* form covalent linkages between the two polymers. Assuming that the radius of gyration of PP-g-MA is about 6.5nm [33], 1.5 times of the  $R_g$  represents approximatively 10nm.

Table 4 : Mean diameter  $d$  and inter-nodule distance  $d_i$  of PP/PP-g-MA/PI (wt%) blends

PP/PP-G-MA/PI	$d$ (nm)	$d_i$ (nm)
80 / 10 / 10	170	160
60 / 20 / 20	250	170
40 / 30 / 30	180	100
20 / 40 / 40	230	95

The results of Table 4 show that  $d_i$  decreases with the addition of polyimide to the blend, from about 160 nm for 10% and 20% of PI, to about 100 nm for 30% and 40% of PI. The calculated values of  $d_i$  are much higher than the  $1.5 \times R_g$  value explained beforehand. However, the PI nodules are randomly dispersed in the polypropylene matrix and some may be separated by a distance small enough for overlapping to occur. Indeed, the TEM images from Figure 7 evidence that even though the polyimide nodules are well dispersed in the whole matrix, there is the presence of some PI nodules' aggregates. In these aggregates, the nodules are close enough to interact with their neighbors which favors nodule/nodule interaction. Such impact of nodules aggregates has been reported in the past, especially in the case of thermoplastic/rubber particles systems [34, 35]. As a result, the physical interactions in the nodule interphase creates a three-dimensional network, which limits the flow of PP chains and thus leads to a secondary storage modulus plateau.

### Mechanical properties

The mechanical properties of the PP/PI blends were investigated by tensile and impact tests. The results are given in Table 5. First, it should be noted that the reference blends containing only PP and PP-g-MA display a decrease in Young's modulus. The more compatibilizer is added to PP, the lower the Young's modulus is. Indeed, PP-g-MA is a maleic anhydride-grafted polypropylene with shorter chains ( $M_n = 36\,000 \text{ g.mol}^{-1}$ ,  $M_w = 91\,000 \text{ g.mol}^{-1}$ ) and with lower crystallinity than PP ( $\theta=42\%$ ), which influences the mechanical behavior of PP by decreasing the Young's modulus, the yield stress and the impact strength and highly increasing the elongation at break.

As expected with the addition of polyimide, there is a noticeable increase in the Young's modulus value for all PP/PP-g-MA/PI blends. The higher the PI content is, the higher the Young's modulus is. The improvement of the Young's modulus compared to the PP/PP-g-MA reference blends varies from

+12% to +35% depending on the PI concentration. This improvement in Young Modulus comes from the high mechanical strength of polyimide. The yield stress is also increased with the addition of PI, with an improvement from the reference blends ranging from +12% to +25% for the highest PI content. The elongation at break is maintained around 65% with the addition of PI up to 30wt%. However, when 40% of PI is added to PP, the presence of many PI nodules act as defects in the material and the elongation at break is diminished to 15%. The impact strength of the blends is maintained at correct values even in the presence of high PP-g-MA contents which usually tends to decrease the material's impact strength. Overall, the mechanical test results indicate that PI has a major impact on the mechanical properties of polypropylene, and that it is an efficient way to improve its Young's modulus.

Table 5 : Mechanical properties of PP/PI blends

PP / PP-g-MA / PI	Young Modulus (MPa)	Yield Stress (MPa)	Elongation at Break (%)	Impact Strength (J/cm <sup>2</sup> )
100 / 0 / 0	1650 ± 30	36 ± 1	47 ± 8	5,7 ± 0,5
90 / 10 / 0	1540 ± 25	34 ± 1	90 ± 9	5,1 ± 0,3
80 / 20 / 0	1485 ± 20	33 ± 1	195 ± 30	4,3 ± 0,4
70 / 30 / 0	1360 ± 20	32 ± 1	330 ± 5	3,4 ± 0,4
60 / 40 / 0	1350 ± 30	31 ± 1	340 ± 10	/
80 / 10 / 10	1730 ± 40	38 ± 0	65 ± 20	4,4 ± 0,4
60 / 20 / 20	1750 ± 35	37 ± 0	75 ± 15	4,8 ± 0,4
40 / 30 / 30	1800 ± 40	39 ± 1	60 ± 10	5,2 ± 0,3
20 / 40 / 40	1820 ± 20	39 ± 0	15 ± 5	/

To corroborate the mechanical properties, DSC experiments were performed and showed that the melting and crystallization temperatures are similar for all the reference and the PP/PP-g-MA/PI blends (thermal properties are displayed in S6). Moreover, the presence of polyimide does not alter the crystallinity rate of the polypropylene phase, which maintains a value of about 50% for all blends. The crystallization temperatures were not modified, meaning that PI has no effect on nucleation or crystallization rate of the PP phase, which further explains the increased mechanical properties. In addition, Wide Angle X-ray Scattering (WAXS) studies was performed, to further analyze the impact of the *in situ* creation of the polyimide phase on the PP matrix crystalline properties (WAXS patterns are displayed in S7). Usually, polypropylene crystalline profile corresponds to the crystalline  $\alpha$ -phase, which is the most common crystalline structure of PP and has the highest thermodynamic stability. In PP/PP-g-MA/PI blends, the same peaks corresponding to the  $\alpha$ -form are present, as well as a new minor peak attributed to the creation of a  $\beta$  crystalline form. This pseudo-hexagonal form is less stable than the  $\alpha$ -form but has a higher heat distortion temperature and impact toughness, which can improve the mechanical properties of the material.

### Thermal properties

Thermogravimetric analyses under a helium and air atmosphere were carried out to determine the influence of the polyimide phase on the thermal stability of PP/PP-g-MA/PI blends. The mass loss as a

function of temperature is presented in Figure 9. The temperatures at 5% and 10% weight loss ( $T_{d5\%}$  and  $T_{d10\%}$  respectively) as well as  $T_o$  (onset temperature degradation) and  $T_d$  (temperature at maximum derivative weight loss), determined from the TGA curves, are reported in Table 6.

The thermal degradation of PP and its blends under helium takes place through a one-step process corresponding to the well described random C-C bond scission mechanism [36] and occurs in the range of temperatures between 375 and 500°C. The onset temperature of decomposition for PP is 430°C and it is shifted for PP/PI blends to more than 450°C depending on the composition. The temperature at 5 % weight loss is also improved in the presence of PI: there is an increase of 25°C for 10 wt% of PI, 30°C for 20 wt % and 34°C for 30 wt% and 40 wt% compared to PP respectively. The addition of polyimide significantly increases the thermal stability of the polymer matrix, and this thermal stability is more pronounced for the highest concentration in polyimide.

*Table 6 : Parameters evaluated from the TGA and DTG curves in helium atmosphere.  $T_{d5\%}$  and  $T_{d10\%}$ : temperatures corresponding to a 5 % and 10 % weight loss.  $T_o$ : onset temperature of degradation.  $T_d$ : temperature at maximal derivative of weight loss.*

<b>PP / PP-G-MA / PI (wt%)</b>	<b><math>T_{d5\%}</math> (°C)</b>	<b><math>T_{d10\%}</math> (°C)</b>	<b><math>T_o</math> (°C)</b>	<b><math>T_d</math> (°C)</b>
<b>100 / 0 / 0</b>	410	423	430	449
<b>0 / 0 / 100</b>	434	449	458	477
<b>80 / 10 / 10</b>	435	446	451	465
<b>60 / 20 / 20</b>	440	451	457	469
<b>40 / 30 / 30</b>	444	456	460	472
<b>20 / 40 / 40</b>	445	456	458	469

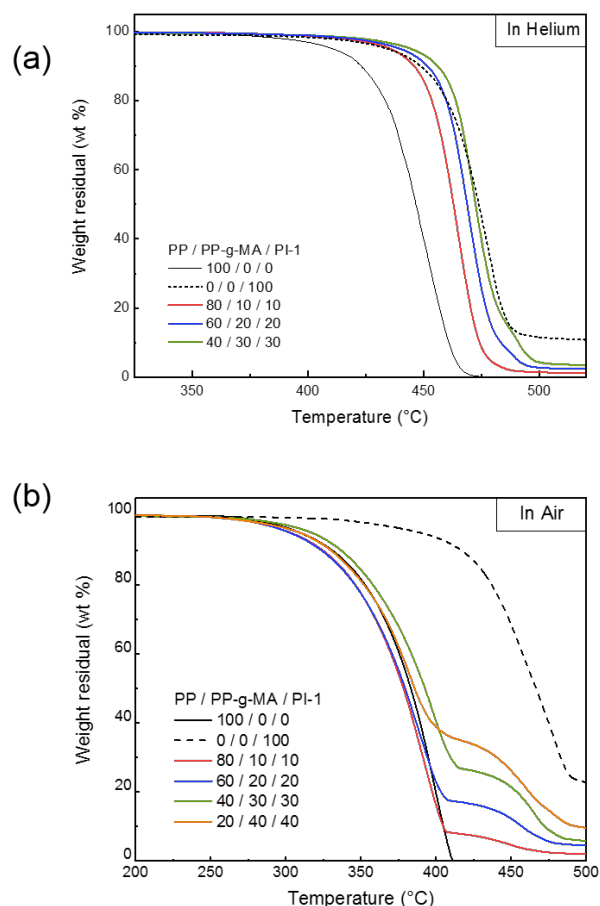


Figure 9 : TGA: of PP, PI and PP/PP-g-MA/PI blends under (a): helium atmosphere, (b): air atmosphere

Thermal degradation of the blends in an oxidizing atmosphere was also studied and is displayed in Figure 9 (b). It can first be noted that the degradation of the materials starts at lower temperatures in air compared to helium. The degradation of PP/PP-g-MA/PI materials occurs in a two-step process: the first step is associated to the degradation of PP and the second step to the degradation of the polyimide fraction. Indeed, the weight residual after 400°C corresponds to the polyimide content in the material. The stability of PP/PP-g-MA/PI blends in air is not significantly improved compared to that of PP.

From the results, the thermal degradation of PP/PP-g-MA/PI blends was not delayed in an oxidizing atmosphere but was significantly improved under helium. The dispersion of a high T<sub>g</sub> polyimide phase in a polypropylene matrix caused this thermal reinforcement. The increase of PP's thermal stability when it is blended with polycarbonate has been reported by Mat-Shayuti *et al.* [4]: these authors observed a 22°C maximum decomposition temperature improvement in a nitrogen atmosphere by incorporating 35wt% of PC in PP. Paszkiewicz and coworkers [7] also worked on PP/PC blends in a twin-screw extruder, and they observed that the incorporation of PC increased the thermal resistance by 20°C in an oxidizing atmosphere. We demonstrated a good thermal reinforcement with the incorporation of PI, as the maximal thermal decomposition temperature was improved by 23°C for 30 wt% of PI. In conclusion, polyimide acts as an efficient thermal stabilizer for polypropylene, delaying the main degradation step of the material. Such stabilization can be interesting for high temperature-based applications.

## Conclusion

In this work we have described a novel method for the preparation of PP/PP-g-MA/PI blends through the *in situ* polymerization of the polyimide phase during extrusion. The synthetic route employed in this study presents several advantages: it is a one-step process, without solvent or formation of by-products.

The polyimide was *in situ* synthesized in the PP/PP-g-MA matrix in a twin screw extruder, and the PI concentration was varied from 10 to 40 wt%. A sub-micrometer dispersion of the polyimide phase was obtained thanks to the *in situ* polymerization, with a mean nodule diameter of 200 nm for all PI concentrations.

Rheological studies showed a significant impact of the polyimide phase on the storage modulus, with the appearance of a secondary plateau at low frequencies, due to a creation of a three-dimensional network. The mechanical strength of PI led to an improvement of the Young's modulus, up to +35% depending on the PI content. The thermal stability of PP was highly improved thanks to the polyimide phase, with an increase up to 35°C for the decomposition temperature at 5 % weight loss.

To conclude, the *in situ* synthesis of a polyimide phase in molten PP by reactive extrusion is an elegant method to associate and modulate the morphology of a high Tg dispersed phase. It led to a very fine and homogeneous nodular dispersion of PI in PP, which is not achievable by classical ways of polymer blending. Other parameters such as dielectric properties or permeability could be explored, to further demonstrate the advantages of blending polyimide with polypropylene.

## Acknowledgements

The authors are grateful to TotalEnergies for the financial support in this project. The authors would like to thank the members of the Centre Technologique des Microstructures de l'Université Lyon1 for their assistance in electron microscopy characterizations. The authors are grateful to Guillaume Sudre for his help with WAXS analysis and the European Synchrotron Radiation Facility (ESRF) in Grenoble for the measurements. The authors would also like to thank the members of the NMR and SEC platform for their help with the experiments.

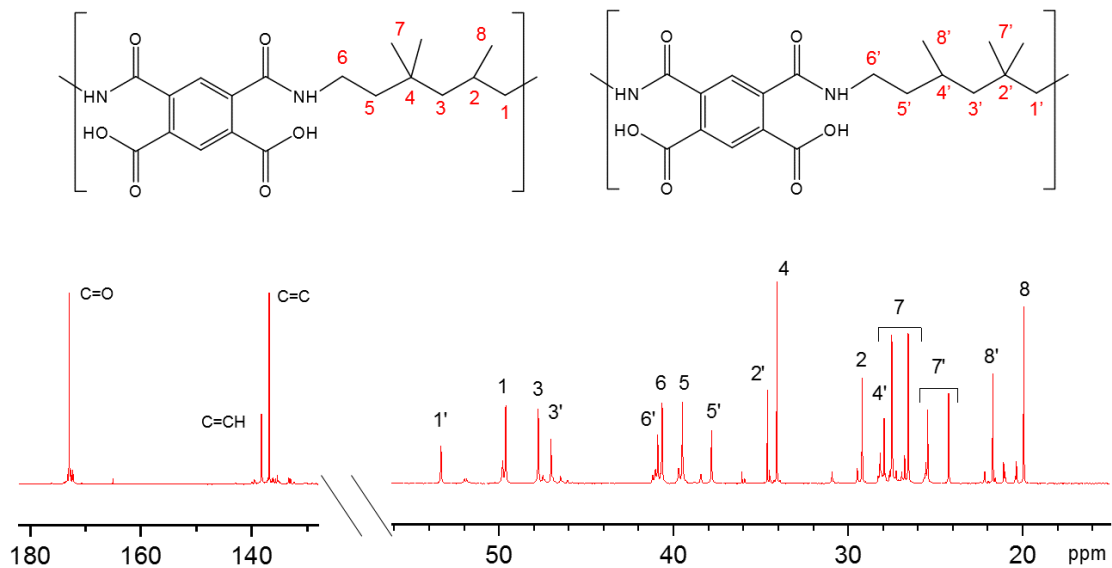
## References

1. Renaut, N., et al., *Fire Retardancy, Thermomechanical and Thermal Properties of PP/PC Blends*. Journal of Macromolecular Science, Part A, 2005. **42**(8): p. 977-991.
2. Matsumoto, K., et al., *Design of a super-ductile polypropylene/polycarbonate blend with high heat resistance by using reactive plasticizer*. Journal of Applied Polymer Science, 2013. **129**(1): p. 443-448.
3. Chand, N. and S.A.R. Hashmi, *Effect of addition of polycarbonate on sheared flow of red mud-filled isotactic polypropylene*. Bulletin of Materials Science, 1999. **22**(4): p. 801-804.
4. Mat-Shayuti, M.S., M.Z. Abdullah, and P.S.M. Megat-Yusoff, *THERMAL properties and morphology of Polypropylene/Polycarbonate/Polypropylene-Graft-Maleic anhydride blends*. MATEC Web Conf., 2016. **69**: p. 03001.
5. Hay, A.S., *Polymerization by oxidative coupling: Discovery and commercialization of PPO (R) and Noryl (R) resins*. Journal of Polymer Science Part a-Polymer Chemistry, 1998. **36**(4): p. 505-517.
6. Oyama, H.T., M. Sekikawa, and S. Shida, *Effect of the interface structure on the morphology and the mechanical, thermal, and flammability properties of polypropylene/poly(phenylene ether)/magnesium hydroxide composites*. Polymer Degradation and Stability, 2012. **97**(5): p. 755-765.
7. Paszkiewicz, S., et al., *Characterization of polypropylene/poly(2,6-dimethyl-1,4-phenylene oxide) blends with improved thermal stability*. Polymer Bulletin, 2018. **75**(8): p. 3679-3691.
8. Jasinska-Walc, L., et al., *Synthesis of isotactic polypropylene-block-polystyrene block copolymers as compatibilizers for isotactic polypropylene/polyphenylene oxide blends*. Polymer, 2018. **147**: p. 121-132.
9. Wei, G.X., et al., *Toughening and strengthening of polypropylene using the rigid-rigid polymer toughening concept Part I. Morphology and mechanical property investigations*. Polymer, 2000. **41**(8): p. 2947-2960.
10. Oyama, H.T., et al., *Drastic improvement in thermal stability of polymer alloys by formation of daughter micelles at the reactive interface*. Polymer, 2018. **137**: p. 107-111.
11. Gao, C., et al., *Fabrication and dielectric properties of poly(ether ether ketone)/polyimide blends with selectively distributed multi-walled carbon nanotubes*. Polymer International, 2015. **64**(11): p. 1555-1559.
12. Liu, X.-Q., et al., *Studies on the Blends of Polyamide66 and Thermoplastic Polyimide*. Journal of Macromolecular Science, Part B, 2010. **49**(4): p. 629-639.
13. Cassagnau, P., V. Bounor-Legare, and F. Fenouillot, *Reactive processing of thermoplastic polymers: A review of the fundamental aspects*. International Polymer Processing, 2007. **22**(3): p. 218-258.
14. Bounor-Legaré, V., F. Fenouillot, and P. Cassagnau, *In situ Synthesis of Inorganic and/or Organic Phases in Thermoplastic Polymers by Reactive Extrusion*, in *Reactive Extrusion*. 2017. p. 179-208.
15. Hu, G.-H., H. Cartier, and C. Plummer, *Reactive Extrusion: Toward Nanoblends*. Macromolecules, 1999. **32**(14): p. 4713-4718.
16. Teng, J., J.U. Otaigbe, and E.P. Taylor, *Reactive blending of functionalized polypropylene and polyamide 6: In situ polymerization and in situ compatibilization*. Polymer Engineering & Science, 2004. **44**(4): p. 648-659.
17. Barroso Gago, L., et al., *Impact of the In Situ Creation of an Epoxy Based Thermosetting Minor Phase on the Physical Properties of a PP Based Blend*. Industrial & Engineering Chemistry Research, 2021. **60**(15): p. 5421-5431.
18. Bahloul, W., et al., *EVA/PBT nanostructured blends synthesized by in situ polymerization of cyclic cBT (cyclic butylene terephthalate) in molten EVA*. Polymer, 2009. **50**(12): p. 2527-2534.

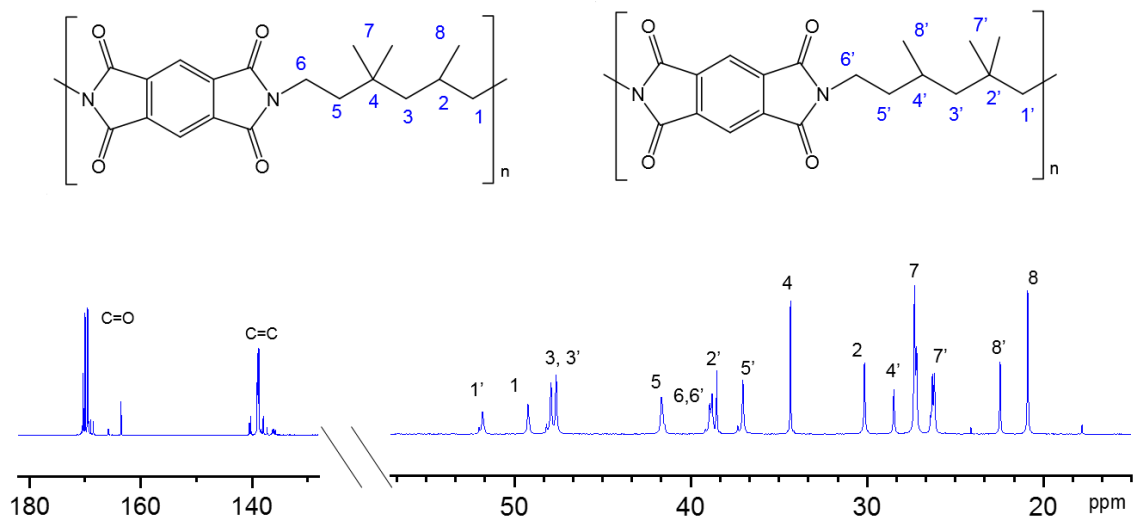
19. Ruzette, A.V. and L. Leibler, *Block copolymers in tomorrow's plastics*. Nature Materials, 2005. **4**(1): p. 19-31.
20. Verny, L., et al., *Solvent-Free Reactive Extrusion As an Innovative and Efficient Process for the Synthesis of Polyimides*. Industrial & Engineering Chemistry Research, 2020. **59**(37): p. 16191-16204.
21. Wang, X.-D., et al., *Crystallization Behavior and Crystal Morphology of Linear/Long Chain Branching Polypropylene Blends*. Polymer Journal, 2008. **40**(5): p. 450-454.
22. Cassagnau, P., et al., *Reactive blending by in situ polymerization of the dispersed phase*. Polymer, 1999. **40**(1): p. 131-138.
23. Kye, H. and J.L. White, *Continuous Polymerization of Caprolactam-Polyether Sulfone Solutions in a Twin Screw Extruder to Form Reactive Polyamide-6/Polyether Sulfone Blends and Their Melt Spun Fibers*. International Polymer Processing, 1996. **11**(4): p. 310-319.
24. Khonakdar, H.A., et al., *Rheology-morphology correlation in PET/PP blends: Influence of type of compatibilizer*. Journal of Vinyl and Additive Technology, 2013. **19**(1): p. 25-30.
25. Codou, A., et al., *Novel compatibilized nylon-based ternary blends with polypropylene and poly(lactic acid): morphology evolution and rheological behaviour*. RSC Advances, 2018. **8**(28): p. 15709-15724.
26. González-Montiel, A., H. Keskkula, and D.R. Paul, *Morphology of nylon 6/polypropylene blends compatibilized with maleated polypropylene*. Journal of Polymer Science Part B: Polymer Physics, 1995. **33**(12): p. 1751-1767.
27. Sailer, C. and U.A. Handge, *Melt Viscosity, Elasticity, and Morphology of Reactively Compatibilized Polyamide 6/Styrene-Acrylonitrile Blends in Shear and Elongation*. Macromolecules, 2007. **40**(6): p. 2019-2028.
28. Sailer, C., et al., *Grafting of polyamide 6 on a styrene-acrylonitrile maleic anhydride terpolymer: melt rheology at the critical gel state*. Rheologica Acta, 2009. **48**(5): p. 579.
29. Moan, M., et al., *Rheological properties and reactive compatibilization of immiscible polymer blends*. Journal of Rheology, 2000. **44**(6): p. 1227-1245.
30. Bhadane, P.A., et al., *Morphology Development and Interfacial Erosion in Reactive Polymer Blending*. Macromolecules, 2008. **41**(20): p. 7549-7559.
31. Jiang, W., S.C. Tjong, and R.K.Y. Li, *Brittle-tough transition in PP/EPDM blends: effects of interparticle distance and tensile deformation speed*. Polymer, 2000. **41**(9): p. 3479-3482.
32. Avril, F., et al., *New Polymer Materials for Steel/Polymer/Steel Laminates in Automotive Applications*. Macromolecular Materials and Engineering, 2013. **298**(6): p. 644-652.
33. Michael, D.W., et al. *Understanding the source of dielectric loss in Titania/polypropylene nanocomposites up to 220 GHz*. in Proc.SPIE. 2017.
34. Bardollet, P., M. Bousmina, and R. Muller, *Relationship between structure and rheological properties in the melt of polymers containing spherical inclusions*. Polymers for Advanced Technologies, 1995. **6**(5): p. 301-308.
35. Bousmina, M. and R. Muller, *Linear viscoelasticity in the melt of impact PMMA. Influence of concentration and aggregation of dispersed rubber particles*. Journal of Rheology, 1993. **37**(4): p. 663-679.
36. Zhang, S. and A.R. Horrocks, *A review of flame retardant polypropylene fibres*. Progress in Polymer Science, 2003. **28**(11): p. 1517-1538.

## Supporting information

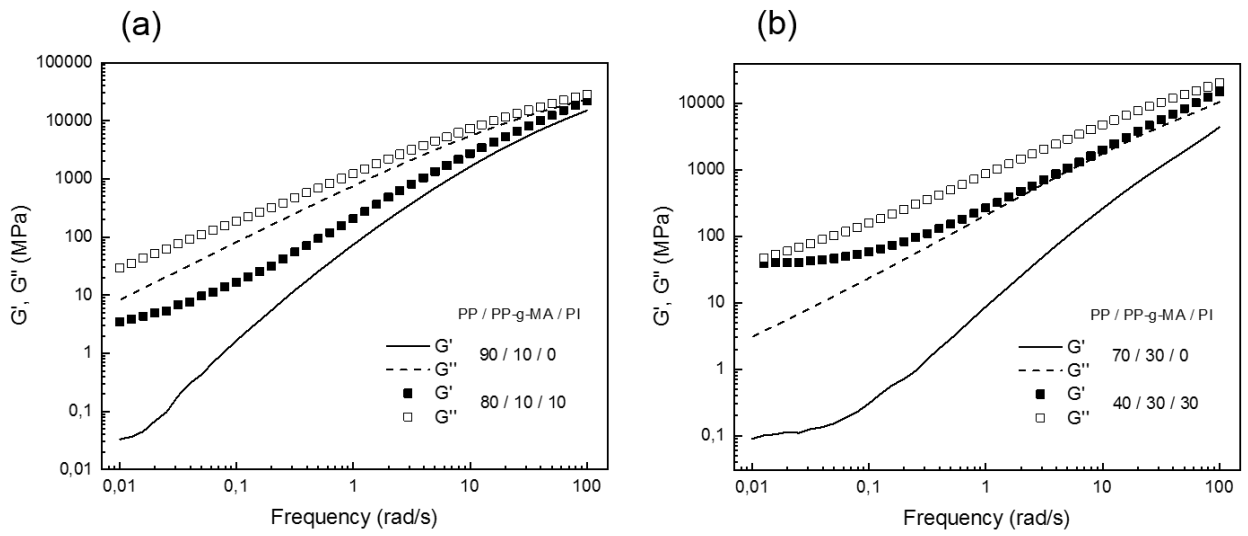
S1 :  $^{13}\text{C}$  NMR spectra of poly(amic acid) and 2: polyimide synthesized in the micro-extruder in HFIP/ $\text{CDCl}_3$  80/20v



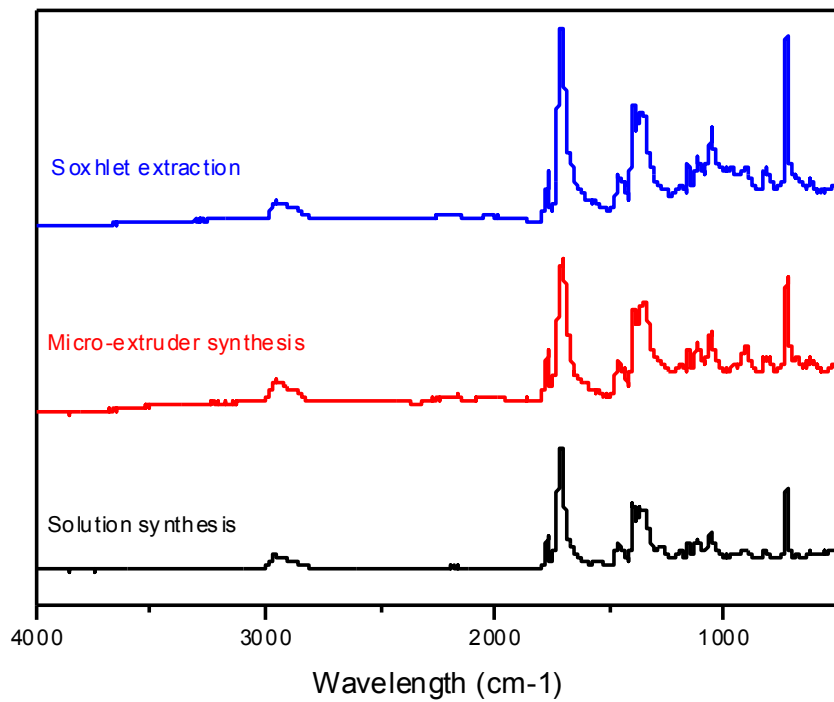
S2 :  $^{13}\text{C}$  NMR spectra of polyimide synthesized in the micro-extruder in HFIP/ $\text{CDCl}_3$  80/20v



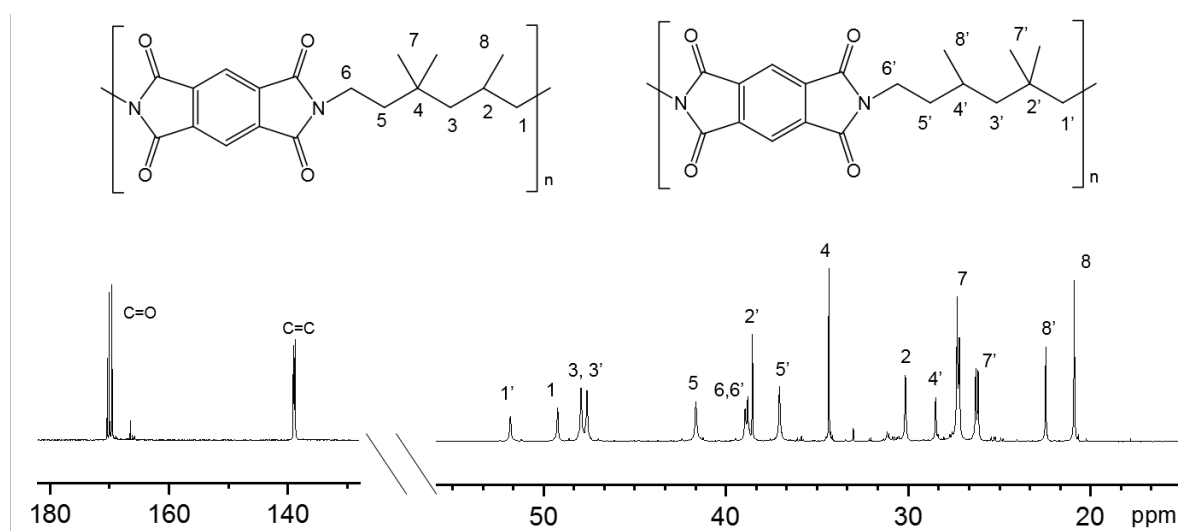
S3 : Storage and loss modulus of PP/PP-g-MA/PI blends (a): 80 / 10 / 10 and (b): 40 / 30 / 30



S4 : FTIR spectra of the polyimide synthesized in solution, synthesized in a micro-extruder, and Soxhlet extracted from an extruded blend.



S5 :  $^{13}\text{C}$  NMR spectra of the Soxhlet extracted polyimide from an extruded blend.



S6: Thermal properties of the blends obtained by DSC

	PP / PP-g-MA / PI	T <sub>m</sub> (PP) (°C)	T <sub>c</sub> (PP) (°C)	ΔH <sub>m</sub> (PP) (J/g)	ΔH <sub>c</sub> (PP) (J/g)	Φ (%)
<b>Reference blends</b>	100 / 0 / 0	163	116	105	105	50.0
	0 / 100 / 0	164	110	87	88	41.7
	90 / 10 / 0	165	113	98	98	46.7
	80 / 20 / 0	164	113	100	101	47.8
	70 / 30 / 0	162	113	100	100	47.8
	60 / 40 / 0	160	114	100	101	48.0
<b>PP/PP-g-MA/PI in situ blends</b>	80 / 10 / 10	165	118	94	93	50.0
	60 / 20 / 20	163	120	86	86	51.7
	40 / 30 / 30	162	121	76	74	52.2
	20 / 40 / 40	162	121	66	63	52.2

S7: WAXS patterns of PP and PP/PP-g-MA/PI blends

